DESIGN OF AN ELECTROMECHANICAL ACTUATION SYSTEM FOR OPTIONAL AUTOPILOT INTEGRATION ON AN ULTRALIGHT AIRCRAFT

TUDOR-GABRIEL-CONSTANTIN GAGIU[1,2], KHALED HACHEM[1,2]
CRISTIAN-TUDOR GHEORMA[1,2]

Abstract. This paper presents the design of an electromechanical actuator system developed to enable autonomous flight control of an ultralight aircraft. The system allows the aircraft to fly autonomously when the pilot releases the controls, while preserving full manual authority at all times. Actuators are installed on all three primary control surfaces – aileron, elevator, and rudder. The core design concept is an overlaid architecture, where the actuator is added to the existing mechanical command chain without replacing it. In manual mode, the pilot operates the controls normally with no added resistance. When the autopilot is activated, a solenoid engages a mechanical coupling that transfers control of the surface to a brushless motor. If power is lost at any point, a return spring automatically disengages the coupling, giving the pilot back full control without any action required. Motor control uses Field-Oriented Control with an absolute position encoder, providing smooth and precise surface movement at the low speeds required for flight control.

Key words: actuator, flight control, optionally piloted vehicle, ultralight aircraft, field-oriented control, electromagnetic coupling, fail-safe, TRL 4.

1. INTRODUCTION

The more electric aircraft paradigm is driving the progressive substitution of conventional hydraulic, mechanical and pneumatic actuation by electrical solutions – electromechanical (EMA) and electro-hydrostatic (EHA) actuators – as part of the wider shift from "fly-by-wire" to "power-by-wire". This transition is expected to yield benefits in overall weight, reliability and safety, together with reduced maintenance, operational and fuel costs [1]. For flight-surface actuation, brushless DC and permanent-magnet synchronous machines are among the most promising motor types,

[1] INCAS – National Institute for Aerospace Research "Elie Carafoli", Bucharest
[2] National University of Science and Technology POLITEHNICA, Bucharest

Ro. J. Techn. Sci. – Appl. Mechanics, Vol. 71, N° 1, P. 67–75, Bucharest, 2026

DOI:10.59277/RJTS-AM.2026.1.04

owing to their high-power density and reliability, and the associated drives are increasingly designed with fault-tolerant and built-in diagnostic capabilities [1]. In the present work the actuator is driven in field-oriented control (FOC); the motor's electrical and mechanical parameters are identified and the controller is configured through the STM32 motor-control tool chain [2].

At INCAS, the ULM testing project targets the development of a TRL 4 EMA test bench for controlled characterization of candidate actuation assemblies. The bench is intended to produce quantitative performance data in support of future qualification campaigns for aerospace-grade applications.

This technical note describes the mechanical and electrical architecture of the bench, the control and measurement chain based on the STM32 B-G431B-ESC1 evaluation board and an independent optical tachometer, and the experimental results obtained during characterization of the T-Motor U5 KV400 / 20:1 planetary gearbox assembly over the full operating speed range up to 5722 rpm [3].

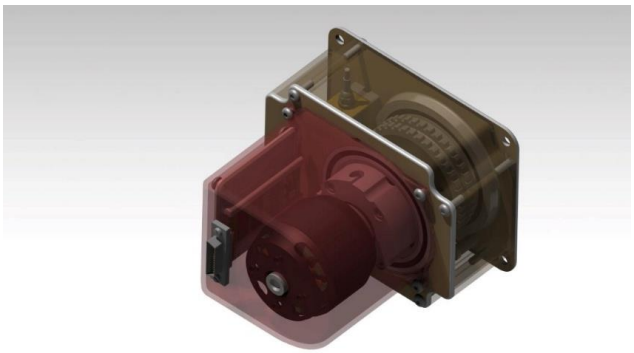


Fig. 1 – Servomechanism render.



Fig. 2 – Picture of servomechanism prototype.

Table 1

EMA assembly component specification

Component	Parameter	Value
T-Motor U5 KV400	KV rating	400 rpm/V
	Max. continuous power	340 W
	Max. continuous current	12 A
Planetary Gearbox	Gear ratio	20:1
	Max. input speed	2000 rpm
B-G431B-ESC1	Controller core	STM32G431 (Cortex-M4)
(ST eval board)	Control algorithm	FOC (field-oriented control)
	PC interface	USB – MotorPilot / MC Workbench
	Data aquation	Real-time via USB
	Gate driver	On-board 3-phase inverter
Solenoid Brake	Hold torque	Solenoid OFF / Solenoid ON
	Actuation type	DC, spring-release
Optical Tachometer	Output signal	TTL pulse train
	Measurement range	0 – 5722 RPM
	Data readout	Dedicated tachometer software (PC)



Fig. 3 –Test bench.

The T-Motor U5 KV400 is a multi-pole outrunner BLDC motor with a KV rating of 400 rpm/V, supplied at 20 V throughout all characterization tests. Coupled to the 20:1 planetary gearbox, the motor shaft speed range of 0–5722 rpm corresponds to a gearbox output speed range of 0–286 rpm.

Motor commutation and speed control are handled by the STM32 B-G431B-ESC1 evaluation board, based on the STM32G431 Cortex-M4 microcontroller with an integrated three-phase gate driver and shunt-based current sensing. The board runs FOC via the STM32 Motor Control SDK, tuned offline in Motor Control Workbench and flashed via ST-LINK/V2.[4] During test runs, speed setpoints are issued and the acquired data (speed, phase current, bus voltage, controller temperature) is logged through the MotorPilot PC application over USB.

Independent speed measurement is performed by an optical tachometer with dedicated readout software on the PC, enabling cross-validation of the ESC internal speed estimator. The solenoid brake, a spring-release DC device at the gearbox output shaft, was tested in both engaged (ON) and disengaged (OFF) states to evaluate its effect on current limit behavior and achievable speed.

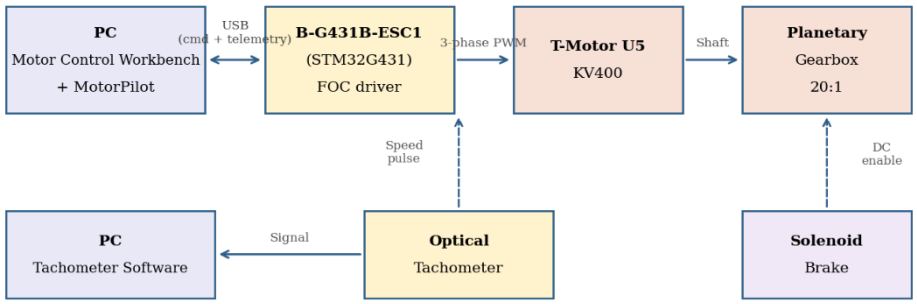


Fig. 4 –EMA test bench signal flow and control chain.

The signal flow is shown in Fig. 1 The PC interfaces with the B-G431B-ESC1 bidirectionally via USB (speed commands and telemetry) and separately reads the tachometer signal through dedicated tachometer software.

2. MEASUREMENT AND CONTROL SETUP

Characterization was performed at 13 speed setpoints: 0, 500, 1 000, 1 500, 2 000, 2 500, 3 000, 3 500, 4 000, 4 500, 5 000, 5 500, and 5 722 rpm (motor shaft). The supply voltage was held constant at 20 V throughout all tests. At each setpoint, phase current and motor speed were recorded from the ESC telemetry stream (MotorPilot) and from the optical tachometer readout, respectively. Tests

were repeated in ascending (acceleration) and descending (deceleration) sequence to capture hysteresis.

Step-response transition times were measured as the time elapsed from setpoint issuance to steady-state speed attainment. The 500 RPM setpoint produced an anomalously large transition time of 7.5 s on the first start-up; this is attributed to the motor's initial magnetization transient from rest and is treated as an outlier in transition time analysis.

At 3 000 rpm a mechanical resonance phenomenon was noted, manifesting as audible vibration of the gearbox housing. This point is flagged in all relevant plots. Additionally, current-limit tests were conducted at maximum speed (5 722 rpm) with the solenoid brake both disengaged (OFF) and engaged (ON), at current limits of 1.0 A, 0.9 A, and 0.8 A.

3. EXPERIMENTAL RESULTS

3. 1. CURRENT–SPEED CHARACTERISTIC

Figure 5 presents the phase current from the ESC telemetry as a function of measured motor speed, for both the ascending and descending setpoint sweeps. The current increases quasi-linearly with speed across the full range, from 9 mA at rest to 781 mA at 5 776 rpm under acceleration, and 770 mA at the same speed under deceleration. The difference between the two curves (current hysteresis) is below 24 mA across all points.

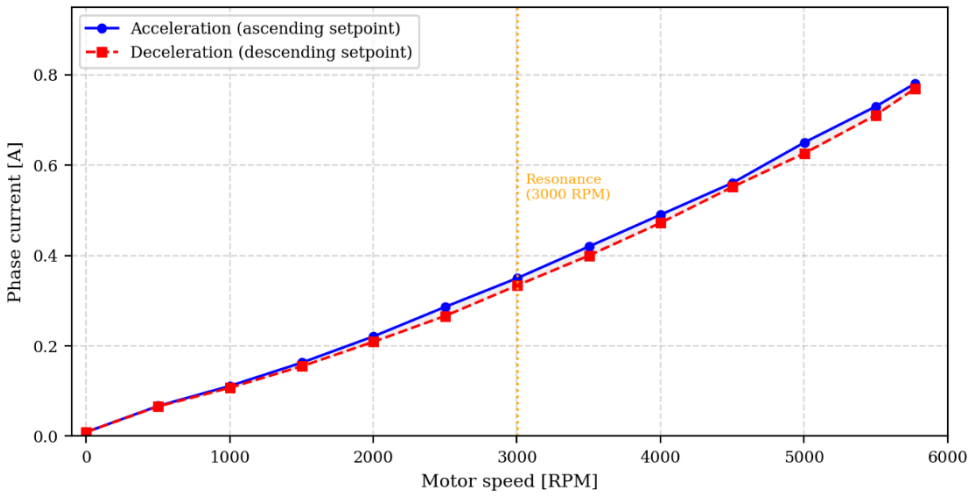


Fig. 5 – Phase current vs. motor speed; T-Motor U5 KV400 / 20:1 gearbox / B-G431B-ESC1.

The linear character of the current-speed relationship confirms that the dominant resistive torque in the assembly (bearing friction, gear meshing losses) is approximately proportional to speed, consistent with viscous friction behaviour. The anomaly at 3 000 rpm, visible as a slight inflection, corresponds to the mechanical resonance noted during testing. No commutation or control anomalies were recorded at this point by the ESC telemetry.

3. 2. SPEED HYSTERESIS

Figure 6 shows the bi-directional speed hysteresis across the full operating range, expressed as the difference between the measured speed in the ascending and descending sweeps at each setpoint

$$\Delta n = n_{asc} - n_{desc} \,. \tag{1}$$

Plotting the difference directly, rather than the two near-coincident speed curves, makes the otherwise imperceptible hysteresis band visible.

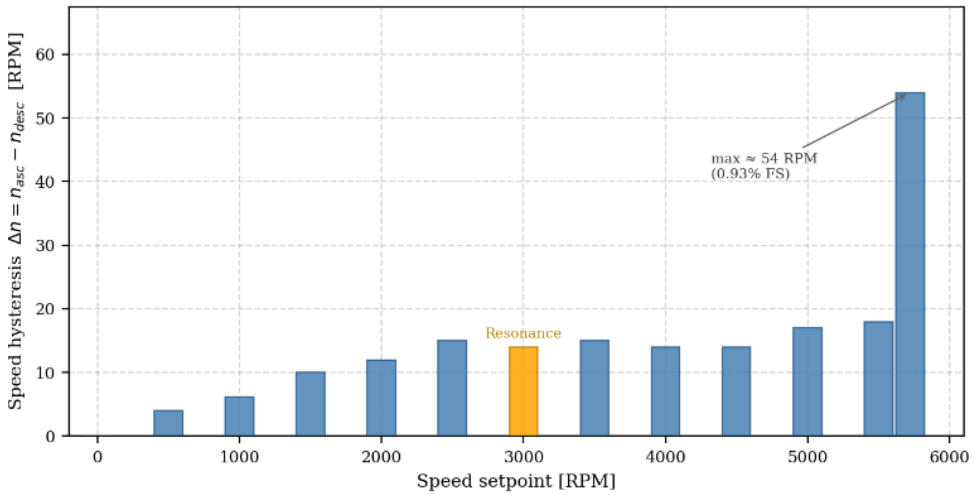


Fig. 6 – Speed hysteresis band vs. setpoint; B-G431B-ESC1 / MotorPilot.

The hysteresis band increases gradually from approximately 4 rpm at 500 rpm to about 18 rpm at 5 500 rpm, remaining below 0.35 % of full-scale speed across the entire normal operating range. The single outlier occurs at the maximum setpoint (5 722 rpm), where the hysteresis reaches 54 rpm (0.93 % of full scale), corresponding to the speed overshoot recorded at the upper limit of the operating envelope. The resonance point at 3 000 rpm does not produce an anomalous hysteresis value, indicating that the resonance affects vibration and settling

behaviour rather than steady-state speed accuracy. Overall, the low hysteresis confirms excellent open-loop tracking of the FOC speed controller.

3. 3. SPEED COMMAND LINEARITY

Figure 7 presents the linearity of the measured speed against the digital RPM setpoint over the full characterization range.

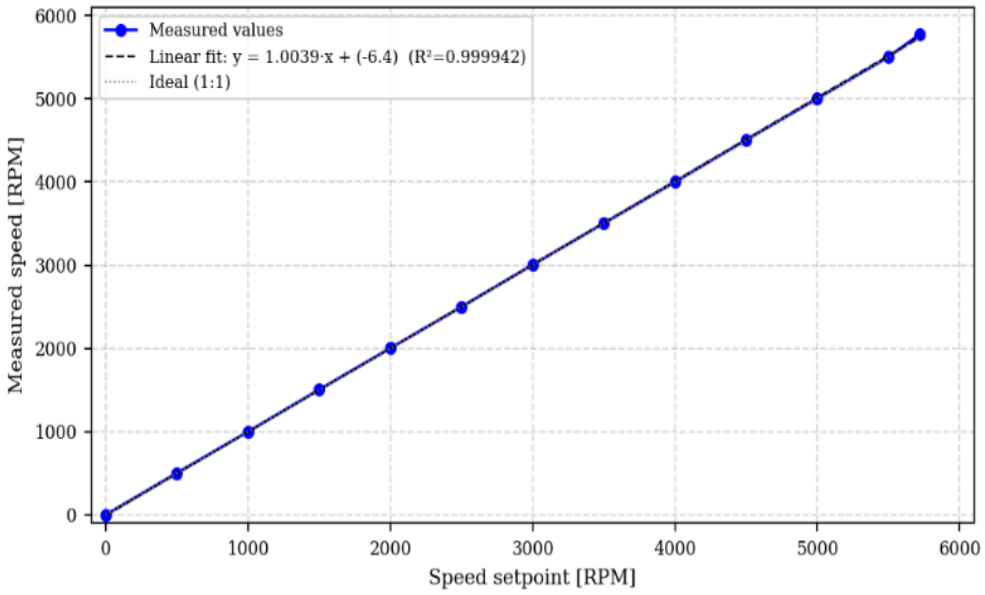


Fig. 7 – Speed command linearity; B-G431B-ESC1 / MotorPilot.

Linear regression over all 13 points yields a slope of 1.0094 and an intercept of − 6.5 rpm, with $R^2 > 0.9999$. The slight positive slope deviation (+ 0.94 %) is traceable to the 5 722 rpm point, where the measured speed (5 776 rpm) exceeds the setpoint by 54 rpm (0.93 % overshoot); all other points fall within 0.5 % of the commanded value. No deadband is observed, consistent with the closed-loop FOC architecture.

3. 4. TRANSITION TIMES AND CURRENT HYSTERESIS

Figure 8 presents the step-response transition times across all valid setpoints (excluding the 500 rpm first-start outlier of 7.5 s) and the point-by-point current hysteresis (difference between acceleration and deceleration current at each speed).

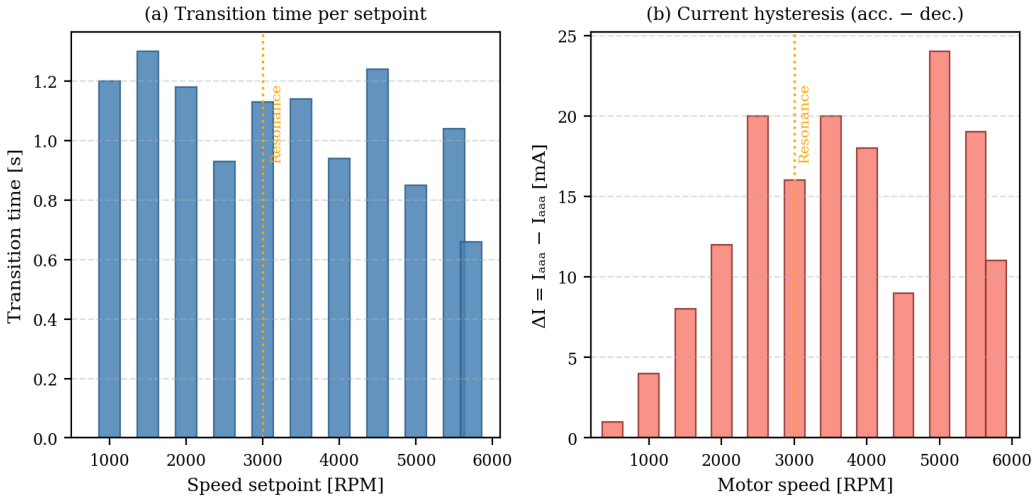


Fig. 8 – Transition times and current hysteresis across the full speed range.

4. DISCUSSION

The characterization results confirm the suitability of the T-Motor U5 KV400 / 20:1 gearbox / B-G431B-ESC1 assembly as a testbed for EMA research. The FOC architecture delivers near-ideal speed command linearity ($R^2 > 0.9999$) and hysteresis below 1 % of full scale across the full 0–5 722 rpm range, without any deadband.

The mechanical resonance at 3 000 rpm warrants further investigation. It manifested as audible structural vibration of the gearbox housing and a slight inflection in the current-speed curve, but did not trigger ESC fault conditions. Possible causes include a gear mesh frequency coinciding with a housing natural frequency, or a rotor imbalance exciting a bearing resonance. A frequency sweep combined with accelerometer measurements on the gearbox housing is recommended to identify and mitigate the resonance mode before high-cycle endurance testing.

The current-limit test results demonstrate that the B-G431B-ESC1 provides effective software-defined torque limiting, a feature relevant for protecting flight control linkages from overload. The 54 rpm overshoot at the 5 722 rpm setpoint (maximum speed) is within acceptable bounds but should be evaluated against actuator mechanical limits in future qualification campaigns.

A rotating torque transducer has been identified as a future procurement item. Its integration will enable direct output shaft torque measurement, allowing mechanical efficiency of the gearbox to be quantified and the ESC current-based torque estimate to be validated against a traceable reference.

5. CONCLUSIONS

A TRL 4 EMA test bench has been developed and characterized at INCAS within the ULM testing project. The bench integrates a T-Motor U5 KV400 brushless motor, a 20:1 planetary gearbox, a STM32 B-G431B-ESC1 FOC controller, and a solenoid brake, with speed measurement from an optical tachometer and parameter logging *via* STM32 Motor Control Workbench and MotorPilot. All characterization was performed at 20 V supply over 13 speed setpoints up to 5 722 rpm.

Key results: (i) near-ideal speed command linearity ($R^2 > 0.9999$) with no deadband; (ii) bi-directional speed hysteresis below 0.5 % of full scale; (iii) transition times in the range 0.66–1.3 s across all setpoints; (iv) quasi-linear current–speed relationship with current hysteresis below 24 mA; (v) effective current-based speed limiting confirmed at 1.0, 0.9, and 0.8 A; (vi) a mechanical resonance identified at 3 000 rpm requiring further investigation.

The bench provides a reproducible testbed for future EMA qualification campaigns and will be augmented with a rotating torque transducer and output-shaft encoder in subsequent phases.

Acknowledgements. This work was supported by a grant of the Ministry of Research, Innovation and Digitization, CCCDI – UEFISCDI, project number PN-IV-P7-7.1-PTE-2024-0248, within PNCDI IV.

Received on June 15, 2026

REFERENCES

1. BOGLIETTI, A. CAVAGNINO, A. TENCONI, A., VASCHETTO, S., TORINO, P. Di, *The safety critical electric machines and drives in the more electric aircraft: A survey*, 35th Annual Conference of IEEE Industrial Electronics, Porto, Portugal; IEEE, Nov. 2009, pp. 2587–2594, doi: 10.1109/IECON.2009.5415238.
2. BERRI, P. C., DALLA VEDOVA, M. D. L., MAGGIORE, P., *Design and Development of an Electromechanical Actuator Test Bench for Validation of Health Monitoring Models*, Proceedings of the 31st European Safety and Reliability Conference (ESREL 2021), Research Publishing Services, pp. 2473–2478, 2021, doi: 10.3850/978-981-18-2016-8_560-cd.
3. *T-Motor Official Store | Drone Motors, ESCs & Propellers for UAVs*, Accessed: Jun. 10, 2026. [Online]. Available: https://store.tmotor.com./
4. *X-CUBE-MCSDK | Product - STMicroelectronics*, Accessed: Jun. 10, 2026. [Online]. Available: https://www.st.com/en/embedded-software/x-cube-mcsdk.html.